

#3

Document Room, ~~EQUIPMENT~~ ROOM 36-412  
Research Laboratory of Electronics  
Massachusetts Institute of Technology

THERMIONIC EMISSION FROM OXIDE-COATED  
TUNGSTEN FILAMENTS

C. P. HADLEY

LOAN COPY

TECHNICAL REPORT NO. 218

DECEMBER 11, 1951

*mg*

RESEARCH LABORATORY OF ELECTRONICS  
MASSACHUSETTS INSTITUTE OF TECHNOLOGY  
CAMBRIDGE, MASSACHUSETTS

The research reported in this document was made possible through support extended the Massachusetts Institute of Technology, Research Laboratory of Electronics, jointly by the Army Signal Corps, the Navy Department (Office of Naval Research) and the Air Force (Air Materiel Command), under Signal Corps Contract No. DA36-039 sc-100, Project No. 8-102B-0; Department of the Army Project No. 3-99-10-022.

MASSACHUSETTS INSTITUTE OF TECHNOLOGY  
RESEARCH LABORATORY OF ELECTRONICS

Technical Report No. 218

December 11, 1951

THERMIONIC EMISSION FROM OXIDE-COATED TUNGSTEN FILAMENTS

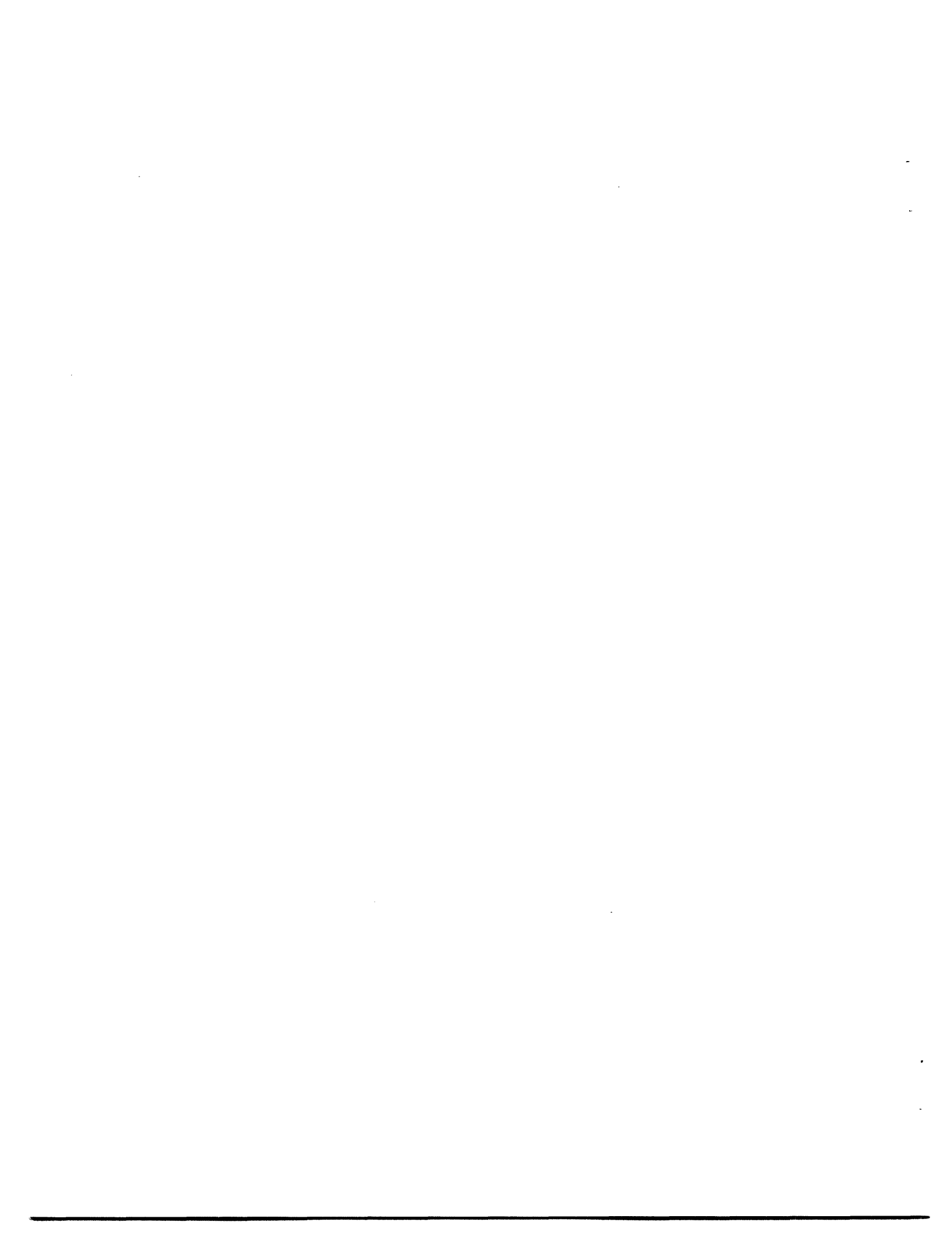
C. P. Hadley

This report is essentially the same as a  
doctoral thesis in the Department of Physics,  
Massachusetts Institute of Technology, 1950.

Abstract

A study has been made of thermionic emission from tungsten filaments cataphoretically coated with alkaline earth oxides. It was found that:

- 1) The emission from the oxide-coated filament was not influenced by the variation of work-function with crystallographic direction of the base metal.
- 2) The apparent deviation of thermionic electrons from Maxwell-Boltzmann statistics was interpreted as due to a potential drop through the coating.
- 3) Such an interpretation led to a method for studying the resistive properties of the coating.



# THERMIONIC EMISSION FROM OXIDE-COATED TUNGSTEN FILAMENTS

## I. Introduction

Although the oxide-coated cathode was reported by Wehnelt (1) as long ago as 1904 and has been studied extensively since then, its properties are still by no means completely understood. An evidence of this lack of understanding is seen in the large number of papers on oxide-coated cathodes which are being published.

During the last fifteen years, modern semiconductor theory has been increasingly applied to oxide-coated cathodes. This theory rests at present on a rather firm foundation, since it has successfully explained many previously unrelated phenomena. For an excess-impurity semiconductor, such as the oxide-coated cathode is believed to be, the physical picture and the energy level structure will be as shown in Fig. 1a,b. Figure 1a shows the cross section of the cathode, while Fig. 1b shows the energy level structure. Two energy bands are indicated. Near the bottom is the filled band, which at absolute zero is filled with electrons. Nearer the top is the conduction band, which is normally empty except for electrons that have been excited. There is a rather wide region separating the top of the filled band and the bottom of the conduction band. Between the conduction band and the filled band are shown the impurity levels that are believed due to a

stoichiometric excess of barium, produced during the activation process. The Fermi level is indicated by  $\mu$  and usually falls about halfway between the impurity levels and the bottom of the conduction band, unless a large fraction of the donor states have yielded electrons to the conduction band. At the outer surface of the oxide coating is shown a potential barrier of height  $F$ , which is called the electron affinity. It represents the difference in energy between an electron at the bottom of the conduction band and an electron well outside the surface. Between the base metal and the oxide proper is shown the interface. It acts as a series resistance between the base metal and the coating proper, and it will affect the electron emission only by the potential drop due to the flow of current.

It is the object of the present work to study the velocity distribution of electrons emitted thermionically from single-crystal tungsten filaments coated cathodically with alkaline earth oxides. The results will be interpreted in terms of the model of Fig. 1a,b.

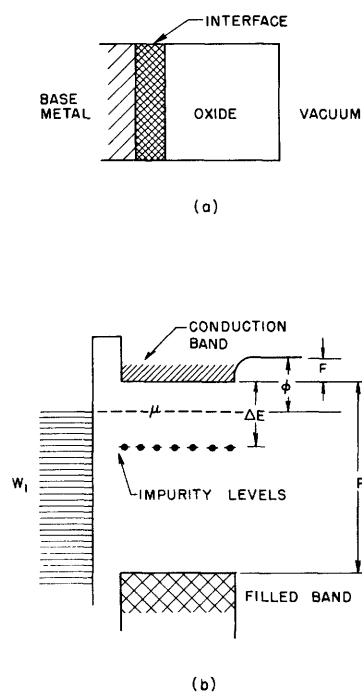


Fig. 1

Model of oxide-coated cathode:  
 (a) physical picture  
 (b) energy levels.

The experimental work to be reported can be divided into four categories:

- a. projection tube studies to assess the effect of the crystallographic structure of the base metal on the emission from the oxide-coated filament
- b. retarding field measurements
- c. accelerating field measurements
- d. x-ray diffraction study of the coating.

## II. Projection Tube Studies

### A. Design of the Tubes

Two projection tubes were used in this study. The two tubes were identical except for minor differences in application of the phosphor.

The envelope of each tube was a 50-mm pyrex cylinder.

The getter was mounted in a side tube and was composed of four Ba-Al pellets mounted in nickel holders. The holders were arranged in a closed circuit so that the getter could be fired with an rf induction heater.

The collector consisted of a 1/4-inch spring, wound of 0.015-inch tungsten wire and stretched between two side-press leads near the edge of the envelope. With such a construction the collector could be outgassed by passing a current through it, yet its diameter was sufficiently large to give a satisfactory collection efficiency. That the collection efficiency was large enough for the purpose was later indicated by the fact that the projection patterns did not vary visibly in intensity either radially or longitudinally.

The inner surface of the tube was coated with a phosphor, ZnS, silver-activated. Good adherence was achieved by means of a binder of potassium silicate.

The emitters used were of bare tungsten wire and oxide-coated tungsten wire. In either case, the emitter was held under tension along the axis of the tube by a tungsten spring made according to the data of Langmuir and Blodgett (2). The ends of the filament were welded to tantalum chips which in turn were welded to the press lead and to the spring.

In both projection tubes, No. 218 tungsten wire was used, designated as Exp. 7767. The wire was originally 0.005-inch in diameter, but it had a somewhat smaller diameter after being mechanically polished to remove the die marks. The polishing procedure, which required about 40 hours, was similar to that which has been described by Johnson, White, and Nelson (3). After the wire had been polished, their diameters were reduced to approximately 0.0045 inch.

The polished tungsten wire was recrystallized in the projection tube by heat. The heating schedule will be described later in connection with experimental procedure.

The carbonate coating was applied to the wire cataphoretically. The suspension used for this process was supplied by the Raytheon Manufacturing Company of Newton, Massachusetts, and was designated by them as C81-5A. It is composed of 1020 g of

triple carbonates (57 percent  $\text{BaCO}_3$ , 43 percent  $\text{SrCO}_3$ , 0.5 percent  $\text{CaCO}_3$ , and a trace of  $\text{MgCO}_3$ ) and 2000 g of carbitol. This suspension was ball-milled for 48 hours, and after the milling, the particle size was approximately  $2.5 \mu$ . Three days before it was desired to coat the wires, the following mixture was prepared: 26.3 percent C81.5A, 43.9 percent carbitol, 10.8 percent distilled water, and 19.0 percent ethyl oxalate. Because of the fact that ethyl oxalate and water react slowly, the suspension was slightly unstable. If the suspension was aged longer than two weeks, the coating produced was no longer smooth.

The wire to be coated was stretched along the axis of a rectangular nickel-plated copper tank which held the suspension. The dimensions of the tank were not important so long as they were large compared to the radius of the wire. A potential difference of 20 volts was applied between the wire and the tank; the tank was made positive with respect to the wire. It was found that the current, for a 0.005-inch wire, 25 cm long, would be originally approximately 50 ma and would drop as the coating formed. A coating time of the order of 1 minute would produce a thickness of approximately 0.001 inch.

## B. Experimental Procedure

The two projection tubes were pumped on a two-stage mercury diffusion system. The baking and outgassing schedule for both projection tubes was essentially the same. Each tube was baked for three periods of three hours each at a temperature of  $500^\circ\text{C}$ , and the McLeod gauge was torched. Between each bake the spring collector was heated to  $1580^\circ\text{K}$  by passing through it a current of 5 amp. Between the second and third bake the bare filament was recrystallized and outgassed, in the manner described below.

In the taking of data, four steps were required.

1. The bare tungsten wire was recrystallized in the projection tube.
2. The tungsten pattern on the projection tube was observed. In order to produce a good pattern, a potential of 4000 volts was applied to the collector and the filament was heated to  $2210^\circ\text{K}$ .
3. The recrystallized tungsten wire was removed from the projection tube, coated cathoretically and returned to the tube. The tube was processed in the same manner as described above and the filament was activated.
4. The projection pattern was again observed.

## C. Experimental Results

### 1. Recrystallization of tungsten wires

The tungsten wires for the two projection tubes were recrystallized by heating with an alternating current, but different time-temperature schedules were used for each. In the first tube, the temperature was raised  $100^\circ$  per hour from  $1800^\circ\text{K}$  to  $2300^\circ\text{K}$ , and then  $100^\circ$  each half-hour to  $2600^\circ\text{K}$ . Finally the wire was flashed at  $2800^\circ\text{K}$  for 5 minutes. The resulting projection pattern showed two single crystals, 2 inches and

5 inches in length, respectively. Using Nichols' data (4), the fact that tungsten is a body-centered cubic structure, and with the knowledge that the crystals form with the 110 direction along the axis of the wire, it was easy to locate the important crystallographic directions. Maxima were observed in the 111 and 116 directions and minima in the 110 and 112 directions. The angles of the maxima and the minima on the projection tube were measured and were found to check calculations within 5°.

In the second tube, the tungsten filament was recrystallized by holding its temperature at 2000°K for 45 hours. At the end of this time the pattern was observed and was found to show approximately six single crystals with numerous faults. The shortest crystal was approximately 1 cm in length. The filament was then flashed for 5 minutes at 2800°K, which removed many of the faults. The pattern could be analyzed, as was done for the first tube, and once again agreement was found with published data.

## 2. Projection-tube studies of oxide-coated filaments

It was impossible in these projection tubes to activate the filaments by using the customary procedures. The final stage in the usual activation process is to draw emission current from the filament with an accelerating voltage such that the current is just space-charge limited. For the smaller currents the space-charge equation is satisfied with a rather small accelerating voltage. With a phosphor, the phosphor potential will remain slightly below that of the filament unless the collector is made more positive than the first crossover point. Since the first crossover point for ZnS is probably of the order of several hundreds of volts, one has no choice but to activate almost completely by heat and to draw current by quite a large accelerating voltage.

The temperature-time schedule for tube No. 1 is given below. The temperatures quoted are computed using the Stefan-Boltzmann relation and an emissivity of 0.25. This will give temperatures correct to within 2 percent over the range used.

Step	Temperature	Time
1	1570°K	0.5 hour
2	1360°K	3 hours
3	1260°K	2.5 hours

It was obvious during the processing that the activation temperatures had been too high. This was shown by the fact that part of the filament glowed more brightly than the rest. The higher temperature was attributed to a deterioration of the surface. Such a deterioration would decrease the surface available to radiate the input power and would result in a higher temperature. Between steps 2 and 3, high voltage was applied to tube No. 1 with the filament at a temperature of 1050°K. With a collector potential of 2000 volts, the anode current was 0.1 ma. It was noted that all the emission came from a small region which was, in fact, the region in which the higher temperatures had been observed. When an attempt was made to increase the current from the apparently inactive regions by increasing the filament temperature, cathode sparking



occurred in the damaged region and in one other isolated region. Eisenstein (5) has attributed the type of sparking observed to a breakdown of the interface and has said that it is more prevalent in cathodes possessing an interface of low conductivity. Evidence to be presented later indicates that the cathodes being used here may have just these properties.

Further activation was attempted on tube No. 1 by heating the filament for 2.5 hours at 950°K. The emission was found to be large from the two regions in which damage to the surface had resulted in a higher temperature. Omitting these regions from the discussion, the emission was quite uniform and no evidence was seen of the crystallographic structure of the base metal.

In tube No. 2, an attempt was made to reduce the damage to the filament by conducting operations at lower temperatures. Accordingly, the following schedule was used: 1190°K for 0.5 hour followed by 1290°K for 34 hours. Even these temperatures were found higher than desirable, for one small region of the filament showed a slightly higher temperature than the rest. On the drawing of emission current above 0.1 ma, sparking occurred in this region. However, it was found possible to get a satisfactory pattern at 0.02 ma. Greater emission was found from one small high-temperature region; but for this, the emission was fairly uniform and showed no influence of the crystallographic structure of the base metal.

### 3. Conclusions

On the basis of the experimental results given on the previous pages the following conclusions may be drawn.

- a. The filaments may be expected to possess an interface of low conductivity.
- b. A uniform emission may be achieved if the filament is handled carefully.
- c. The emission cannot be seen to be affected by the crystallographic structure of the base metal.

## III. Emission Studies

### A. The Experimental Tube

#### 1. General features

The tube with which quantitative emission studies were made was a diode of concentric cylindrical geometry. A drawing of the important parts of the tube is shown in Fig. 2. The emitter was an oxide-coated tungsten filament. The anode was of the usual guard-ring construction, but possessed the unusual feature of being movable. The purpose of this was to be able to move the anode away from the central coated portion of the filament during activation and thus to prevent anode contamination. For the activation the current was collected by an auxiliary anode. During measurement the sliding anode was moved over the oxide coating.

Because of the use of a filament emitter and a sliding anode, it was necessary for three of the leads to go the length of the tube in order to reach the press leads. These

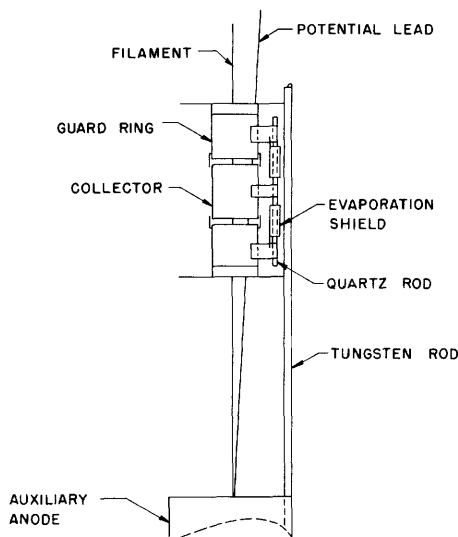


Fig. 2  
Anode structure.

three leads were: one end of the filament, one of the two potential leads that are attached to the filament at the edge of the filament coating, and the lead to the collector portion of the sliding anode. In order to eliminate polarization effects, it was necessary that the collector system should not "see" any dielectric which is also viewed by the filament system. This requirement was partially satisfied by tantalum shields which enclosed the conductors to the bottom of the filament and the lower potential lead. In the experimental work to be described later, polarization currents of the order of  $10^{-14}$  amp were found. Consequently, emission currents below  $10^{-13}$  amp were considered un dependable and were discarded.

### 2. The sliding anode

The sliding anode consisted of a collector and two guard rings. These were three cylinders, 1.59 cm in diameter, made of 3-mil tantalum sheet. The length of the collector was 1.63 cm. The three cylinders were held rigidly by three quartz rods. In order to decrease leakage, each of the quartz rods was protected from foreign deposits by two evaporation shields. To prevent electrons from passing out of the collector system, each of the guard rings had a collar to shield the space between the guard ring and the collector. The extreme end of each guard ring was fastened rigidly to a tantalum disk. These disks had a diameter such that they rested lightly on four 70-mil tungsten uprights. It was on these uprights that the anode structure rode, and the guard rings were grounded by contact between the disks and the uprights. Contact to the collector was made through a flexible nickel spiral.

### 3. The filament structure

The filament base metal was of No. 218 tungsten wire, polished and recrystallized as was described in section II. After polishing, the bare filament had a diameter of 4.68 mils. The section of the filament within the auxiliary anode was cataphoretically coated, by using the method described in section II, to a diameter of 8.41 mils.

Special provisions were made so that the temperature over the emitting section of the filament would be uniform. The distance from the central section of the filament to the spring at the bottom of the tube was 20.5 cm. The data published by Langmuir, McLane, and Blodgett (6) on tungsten wire have indicated that this length is sufficient to assure that, even at temperatures as low as 500°K, the temperature of the filament under the collector was constant to at least 3°C. The top of the filament was welded to a 10-mil tantalum wire 6.4 cm long, which in turn was welded to the press lead.

If the properties of tantalum are compared with those of tungsten, it is found that tantalum has a slightly smaller total emissivity, a larger resistivity, and a heat

conductivity which is smaller by a factor of nearly 3.7. This information, combined with the Langmuir, McLane, and Blodgett data on tungsten, indicates that 6.4 cm of 10-mil tantalum is roughly equivalent in temperature distribution to 18 cm of 5-mil tungsten wire. On the basis of these considerations it is concluded that the temperature of the filament under the collector was constant to 3°C.

The temperature of the filament was measured by comparing its resistivity with the published values (7) of resistivity as a function of temperature. The current was determined by measuring with a potentiometer the potential drop across a series 1-ohm resistance. The potential drop over the central section of the filament was measured between two potential leads which were separated by 7.53 cm.

The resistance of a wire of length  $L$ , diameter  $d$ , and resistivity  $r(T)$  is given by

$$R = r(T) \frac{4L}{\pi d^2}. \quad (1)$$

Assuming the data for  $r(T)$  to be correct, the error in  $T$  depends on the geometrical factor  $L/d^2$ . The length  $L$  was measured with a cathetometer and was accurate to 0.5 percent, while  $d$  was measured with a calibrated microscope and might be in error by 2 percent. The factor  $L/d^2$  may therefore be incorrect by as much as 5 percent. An error of 5 percent in  $L/d^2$  could cause a temperature error of as much as 20° at 500°K. This difficulty was overcome by the following procedure. By using Eq. 1 and the data for  $V$  vs  $i$ , a plot was made of temperature as a function of current. The curve was extrapolated to zero current, and the extrapolation was found to be slightly different from the measured room temperature. The constant  $L/d^2$  was adjusted until the extrapolation agreed with room temperature, and the  $T$  vs  $i$  curve was replotted. It was estimated that temperatures could be read from this final curve to within 2°C.

#### 4. The getter

The getter consisted of four Ba-Al pellets mounted in four tantalum holders. The tantalum was pre-outgassed at 1550°C for one-half hour. The holders were welded together in a ring, in order that the pellets might later be fired with the induction heater, and were mounted in an appended getter bulb. The tubing which joined the getter bulb to the main tube was formed in such a manner that the barium released during firing could not reach the main tube by rectilinear motion.

#### 5. General details of construction

All the metal parts of the tube were joined together with the spot welder. In most cases copper electrodes were used, and the copper was subsequently removed by washing in warm dilute nitric acid for 5 to 10 minutes. For some of the parts (notably the getter holders and the filament) washing with nitric acid would have been impossible, so molybdenum electrodes were used in the welder. Before they were assembled in the main tube, all of the metals were outgassed in a dummy tube at temperatures ranging from 1650°C to 1750°C.

The glassware was cleaned with soap and water, distilled water, dichromate cleaning

solution, and again with distilled water. After the final cleaning, neither the metal parts nor the inside of the glass envelope were touched with the hands except when wearing white cotton gloves.

#### 6. Processing of the tube

The tube was evacuated on a two-stage mercury diffusion system backed by a Welch roughing pump. The pressures were measured with a Bayard-Alpert ionization gauge. The evacuation was accompanied by the usual schedule of alternate bakes at 500°C and heating of the metal parts by induction. Because of the presence of the quartz rods, it was considered unwise to heat the main anode above 1200°C. Previous work had shown that tantalum which had been pre-outgassed at temperatures above 1500°C for several hours could be well outgassed later at temperatures as low as 1200°C. It was feared that at these temperatures the sliding anode, even though it were away from the oxide, might become contaminated during conversion and activation. It was found later, however, that the thermionic emission data showed no evidence of dirty anodes.

During the conversion of the carbonates of the coating to the oxides, the liquid air on the trap was replaced by a slush of acetone and dry ice. The temperature of the filament was raised slowly and held over a period of 5.5 hours at 950°K. During this time the pressure rose from  $10^{-9}$  to  $10^{-7}$  mm Hg. The temperature of the filament was held at 950°K for 2.5 hours while the pressure slowly fell. When the pressure had remained steady for 1 hour at  $3.5 \times 10^{-8}$  mm, the conversion was assumed completed and the temperature was lowered. With the tube cold, the pressure was  $5 \times 10^{-9}$  mm Hg.

When the filament was being activated the auxiliary anode was made positive by 1.5 volts. The filament temperature was raised over a period of 2 hours to 900°K, and was held at this temperature for 3.5 hours. During this time the anode current rose from  $1.2 \times 10^{-7}$  to  $1.2 \times 10^{-6}$  amp. At no time during the activation did the pressure rise above  $10^{-8}$  mm Hg.

The getter was outgassed for 1 hour at red heat and was then fired. The constriction was warmed very slowly, and the tube was removed from the system.

The filament was seasoned for 93 hours by drawing current with the temperature at 800°K. During this time the anode current slowly rose, and as it rose the collector voltage was increased from 1.5 to 16.5 volts. At the end of 69 hours the current had increased to  $2 \times 10^{-4}$  amp and remained constant at that value for 24 hours. Before thermionic data were taken, the leakage resistance was measured between the collector and the filament and was found to be greater than  $10^{14}$  ohms.

#### B. The Measuring Circuit

The measuring circuit used in this part of the work is shown in Fig. 3. It was identical, except for minor changes, to one used by Nottingham (8,9) in his work on tungsten and thoriated tungsten. The operation of the circuit will be described briefly.

The two thyratrons (FG-67) were fired alternately by signals which were applied to their grids 180° out of phase. Because of the coupling condenser between the plates,



one thyatron was turned off when the other fired. The pulse of current through either thyatron was as pictured below. The current through the right thyatron also passed



through the filament of the experimental tube and through the filament of an auxiliary tube. During the pulse of current, the filament was thrown positive with respect to its collector by as much as 40 volts. Consequently no anode current was being collected.

After the pulse, however, the filament potential dropped to a value determined by the potentiometer arrangement shown in the lower right-hand part of Fig. 3. The current collected between pulses was therefore characteristic of the voltage supplied by the potentiometer.

The auxiliary filament, which was heated by the same current which heated the main filament, was viewed by an FJ-114 phototube. The output of the phototube was amplified by an FP-54 electrometer tube. The galvanometer in the output of the FP-54 was used as a null device by means of the bucking voltage in the FP-54 grid circuit. Any change in the galvanometer reading was indicative of a change in temperature of the filament of the main tube. The value of the filament temperature could be determined by finding what direct current through it was equivalent, in its effect on the phototube, to the pulsating current.

The plate voltage of the thyatrons was supplied by a motor generator which was usually run near 600 volts. Since the output of the generator changed from time to time, an automatic regulating device was needed. The regulation was supplied by two 6SN7's connected in parallel with the field coils of the generator. The grids of the 6SN7's were in the output of the FJ-114 phototube. A beam of light from the galvanometer in the FP-54 plate circuit passed through a wedge-shaped aperture which was focused by lens C on the FJ-114. A change in temperature of the auxiliary filament (and hence of the main filament) caused a change in the signal to the grids of the 6SN7's. The resulting change in the plate current of the 6SN7's was in such a direction as to correct the generator voltage, the variation of which presumably caused the original temperature change. The automatic regulation was supplemented by a manually controlled resistance in series with the generator field rheostat. With the combination of automatic and manual control, one could hold the filament temperature constant, during measurement, to within a tenth of a degree.

The collection current was measured with a Compton electrometer which had a sensitivity of 2 mm/mv. For the larger currents, 7 resistances were used which had values ranging from  $10^6$  ohms to  $10^{10}$  ohms. For the smaller currents, the accumulation of charge method was used.

The repetition frequency of the thyatrons was 100 cps. In the interest of stability it was desirable that the current pulse through a thyatron should not be turned off during the rapidly decreasing part of the current waveform. Accordingly, the time constant in the plate circuit of the thyatrons was made approximately  $8 \times 10^{-4}$  seconds. At 100 cps each thyatron had approximately 6 time constants to approach equilibrium.

The grids of the thyratrons were actuated with a differentiated square wave. A Hewlett-Packard audio oscillator operating at 100 cps was applied to the input of a General Radio square-wave generator. The output of the square-wave generator supplied an audio transformer. The output of the transformer provided push-pull signals to two audio amplifiers which passed on the signals to the two grids of the thyratrons. The circuit constants of the audio amplifiers were such that the square waves became differentiated, and sharp positive peaks of voltage were available to fire the thyratrons. With this arrangement, extreme stability in pulse widths was achieved.

The pulsing circuit was used for measurements in which the anode-to-cathode voltage of the experimental tube was in the range of less than 12 volts accelerating. For accelerating voltages greater than this the potential drop along the filament became unimportant, and direct-current heating was used. The accelerating voltages were supplied by dry cells and by a regulated power supply.

The bucking voltages of the Compton electrometer, of the FP-54, and the potential drop along the filament were measured by a Leeds and Northrup type-K potentiometer. The filament current was measured by determining, with the Leeds and Northrup potentiometer, the potential difference across a standard 1-ohm resistance in series with the filament.

### C. Richardson Data

Data for the Richardson plot shown in Fig. 4 were obtained using a collection potential of 10.5 volts and temperatures running from 420°K to 660°K. The highest current density used was less than  $2 \times 10^{-7}$  amp/cm<sup>2</sup>. Even at the higher currents no change in the state of activation of the filament could be noted.

It is shown later that Schottky plots were satisfactorily explained by the strip theory of patches for  $a = 0.2$  volt and  $z_0 = 2 \times 10^{-6}$  m. A Richardson plot of emission from a patchy surface will yield an effective work-function which we may define from the following considerations.

Let

- $s_i$  = area of the  $i^{\text{th}}$  patch
- $A_i$  = A-value of  $i^{\text{th}}$  patch
- $\phi$  = work-function of  $i^{\text{th}}$  patch
- $S$  = total emitting area
- $A$  = effective A-value
- $\phi$  = effective work-function.

Then  $A$  and  $\phi$  are defined by the equation

$$\sum_i s_i A_i T^2 \exp - \frac{e\phi_i}{kT} = SAT^2 \exp - \frac{e\phi}{kT}. \quad (2)$$

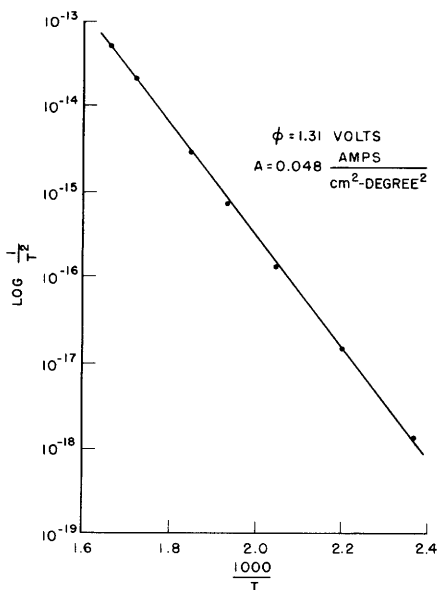


Fig. 4  
Richardson plot.

If the various values of  $s_i$  and  $A_i$  were nearly equal, then the effective work-function would be nearly that of the lowest value of  $\phi_i$ . It is also recalled that the  $\phi$  determined by a Richardson plot will contain a temperature-dependent term, and  $A$  will contain a term involving the temperature dependence of the work-function.

From the slope of the best straight line through the points of Fig. 4, and from the computation of the intercept of this line, the effective values of the work-function and the  $A$ -value turned out to be

$$\phi = 1.31 \text{ volts}$$

$$A = 0.048 \text{ amp/cm}^2 \text{ - degree}^2.$$

It is worthwhile to compare these results with those found by other workers. Blewett (10) gives typical results for oxide-coated cathodes of  $\phi = 1.1$  volts to 1.4 volts and  $A = 0.01 \text{ amp/cm}^2 \text{ - degree}^2$ .

Mahlman (11) found  $\phi$  varying between 1.33 volts and 1.47 volts and  $A$  about  $0.03 \text{ amp/cm}^2 \text{ - degree}^2$ . Mutter (12) gives  $\phi = 1.39$  volts and  $A = 0.0058 \text{ amp/cm}^2 \text{ - degree}^2$ . These figures from Mutter are quoted for a well-activated cathode before subsequent poisonings and attempts at reactivation with methane and with barium evaporation.

In comparing these results quoted from other workers with those found in the present work, one concludes that the present values are by no means out of line, but nevertheless are such as to indicate a somewhat low state of activation.

#### D. Retarding Potential Data

The retarding field measurements were made for temperatures between 514°K and 583°K. The current densities were even lower than those used for Richardson data, and no change in the state of activation of the filament was noted during the whole series of runs.

Currents below approximately  $10^{-13}$  amp were found not reproducible, because of polarization currents in the glass walls of the tube and other insulators. With the filament cold, the filament potential was changed suddenly from 0 volt to -12 volts. Over periods of several hours after that, a slowly decreasing current of the order of  $10^{-14}$  amp was observed. This current was in the direction of electron flow from the filament to the collector. If the filament potential were changed from a negative to a positive value, a reverse current was found. Since these currents were not dependent on voltage, but rather on the change of voltage, they could not be attributed to leakage. It proved impractical to wait for the polarization currents to stop before making a measurement of electron current. Consequently currents less than  $10^{-13}$  amp were considered in



error by as much as 10 percent and were discarded.

The experimental retarding curves are shown in Figs. 5, 6, 7, and 8, with the logarithm of the current plotted as a function of  $500 V/T$ . The Schottky (13) theory predicts that the current under these conditions would be given by

$$J = \frac{2}{\sqrt{\pi}} J_0 \left[ \sqrt{\frac{\epsilon V}{kT}} e^{-\frac{\epsilon V}{kT}} + \int_0^{\infty} e^{-x^2} dx \right] \quad (3)$$

Here all symbols have the usual meaning. This equation is plotted as the solid line in Fig. 9. The dotted line of Fig. 9 is the modification of the Schottky theory by the reflection factor found by Nottingham (8) for tungsten and thoriated tungsten. One finds very considerable differences between the present experimental data and either curve of Fig. 9. In the first place, if a typical curve (Fig. 8, for example) is compared with Fig. 9, it will be found that the experimental curve is tremendously more rounded than would be predicted by the Schottky theory or by the Schottky theory combined with Nottingham's reflection coefficient. In the second place, even at low currents, the curves have a smaller slope than that predicted by retarding potential theory. Thirdly, the curves are displaced toward accelerating potentials. If one extends the two straight-line portions of Fig. 8 and defines the intersection as zero-field, zero-field comes at about 5.2 volts. If the work-function of tantalum is taken as 4.1 volts, the cathode work-function would have to be -1.0 volt. All of these anomalies must be resolved by any mechanism which is proposed to explain the data. Since Fan (14) and Hung (15) have demonstrated that the electrons emitted thermionically from oxide-coated cathodes have a Maxwell-Boltzmann distribution in energy and are in temperature equilibrium with the cathode, we must look to some other explanation of this phenomenon.

As an approach to the problem of the anomalous curves, let us consider the various deviations of an experimental tube from ideal conditions.

1. Nonconcentricity of anode and cathode. Let us consider the most extreme condition of nonconcentricity in which the cathode is very near to the anode. For most of the cathode area the retarding potential data would behave as for plane-parallel geometry. Therefore, retarding potential curves under these conditions would be expected to show less rounding, not more.

2. Space charge. Application of the space-charge theory of Langmuir (16) indicates that effects should be negligible for collection currents as small as have been used here. This is borne out experimentally by the Richardson plot of Fig. 4, where a straight line is found up to temperatures of  $660^\circ\text{K}$ ,  $80^\circ$  higher than the greatest temperatures used for the retarding potential plots.

3. Variation of temperature along the emitter. To test the effect of such a variation one may assume a model in which half the cathode is at  $550^\circ\text{K}$  and half is at  $560^\circ\text{K}$ . This temperature difference is several times that estimated to exist along the cathode.

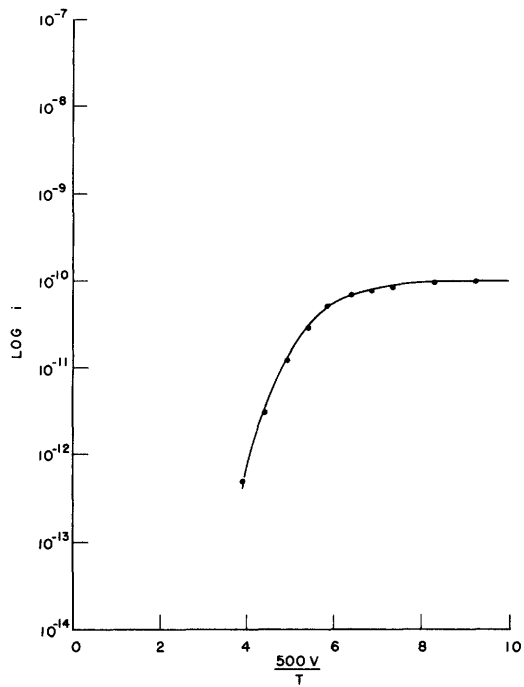


Fig. 5  
Retarding potential plot (pulse).  
 $T = 514.2^{\circ}\text{K}.$

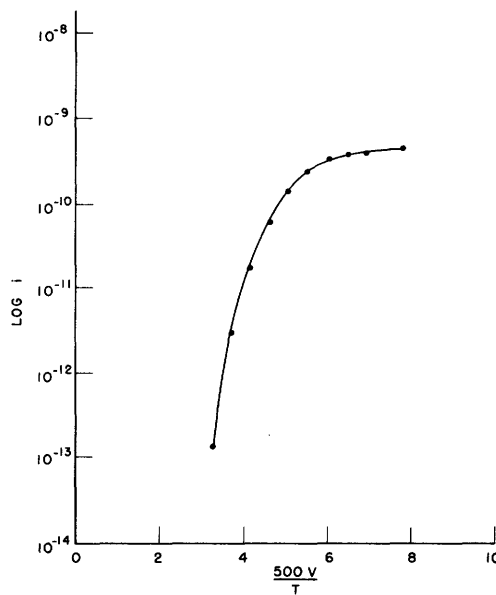


Fig. 6  
Retarding potential plot (pulse).  
 $T = 536.2^{\circ}\text{K}.$

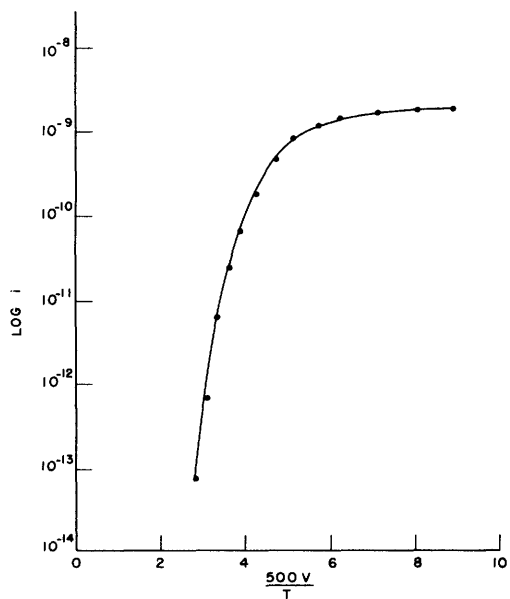


Fig. 7  
Retarding potential plot (pulse).  
 $T = 563.2^{\circ}\text{K}.$

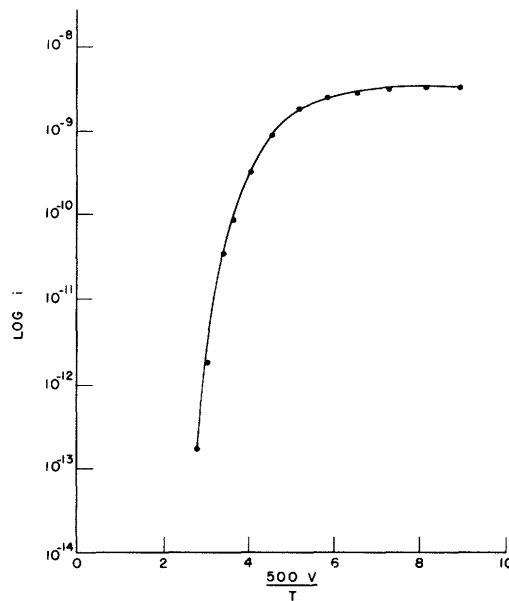


Fig. 8  
Retarding potential plot (pulse).  
 $T = 582.5^{\circ}\text{K}.$

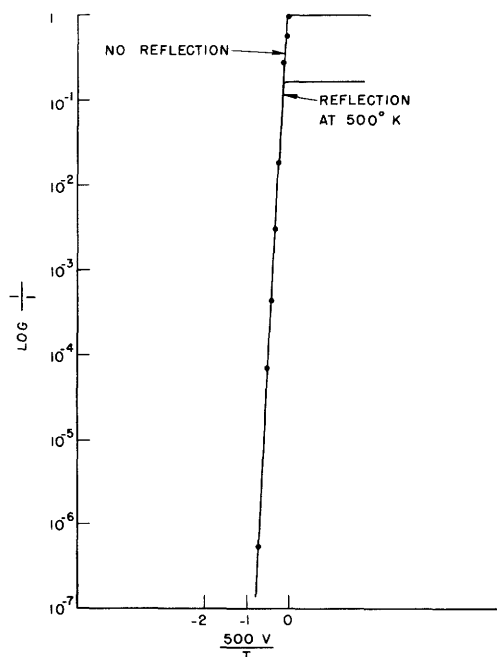


Fig. 9

Schottky retarding potential, theory.

If the currents from the two areas are added, and the total current is plotted as a function of  $500 V/T$ , the result gives a curve whose shape cannot be distinguished from that of the theoretical curve of Fig. 9. Since the temperature variation along the experimental cathode has been estimated to be no more than  $3^\circ\text{C}$ , this variation cannot explain the shape of the retarding potential curves.

4. Potential drop along the filament. If the pulsing circuit were not operating correctly, both the rounding of the curves and the displacement to higher voltages might result. To prove that this effect is not present, the following experiment was performed. A retarding potential plot was made, using dc heating. This plot is shown in Fig. 10. Using a pulse curve at the same temperature, a graphical integration was performed (extending over the potential drop

of the directly heated filament) to give a simulated dc curve. The simulated curve is plotted in Fig. 11. It will be noted that the actual dc curve has a current twice as large as the simulated curve. This is to be expected, for the simulated curve is derived from the pulse curve in which current is being collected only half the time. Furthermore, the dc curve is shifted to the right with respect to the simulated curve by about 0.3 volt. This voltage represents the drop, under dc heating conditions, from the center of the emitter to the point of application of the retarding voltage and is to be expected. When the necessary vertical and horizontal translations are made, the two curves are seen to fit well (Fig. 12). It must be concluded that no difficulty exists as a result of a potential drop along the filament.

5. Anode effect. Clean tantalum anodes have been found to show negligibly small anode effect (15). This was found true in the present case by suddenly changing the filament potential so as first to collect saturation current and then to collect a much smaller current. As long as the currents were above the polarization current region, no time effects were observed.

6. Patchy anode. It is usually found that anodes in oxide-coated cathode studies become patchy by showing areas of smaller-than-normal work-function. The principal result of this is that the retarding potential curves show tails and shifts to lower potentials. No tails are found on the experimental curves of Figs. 5 to 8, and the shifts are toward higher, not lower, potentials. If the shifts were to be attributed to higher work-function patches, a large fraction of the anode would have to have a work-function of the

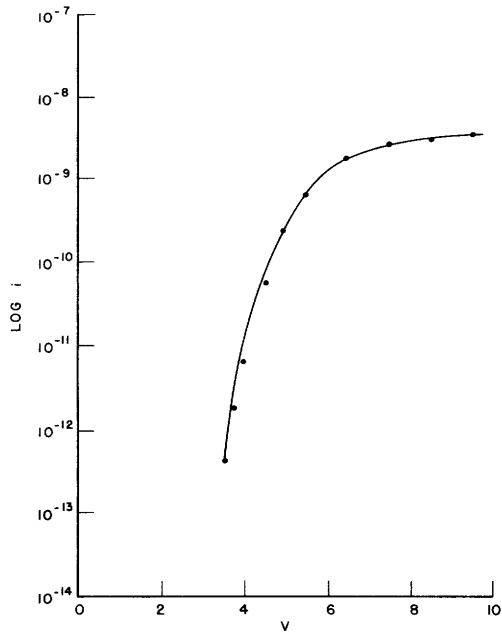


Fig. 10  
Retarding potential plot (direct current).  $T = 563.2^{\circ}\text{K}$ .

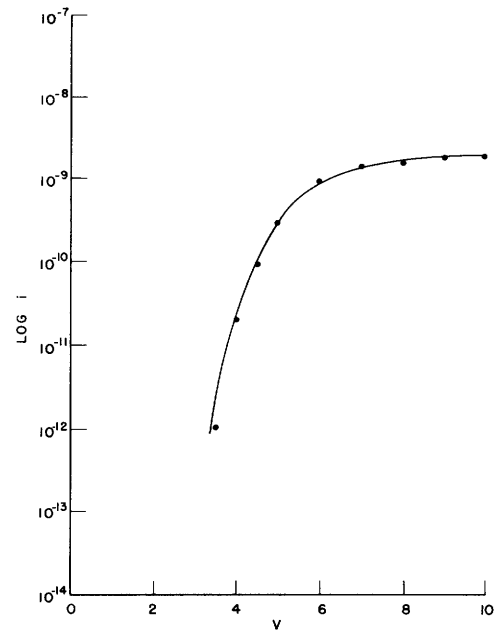


Fig. 11  
Retarding potential plot (simulated direct current).  $T = 563.2^{\circ}\text{K}$ .

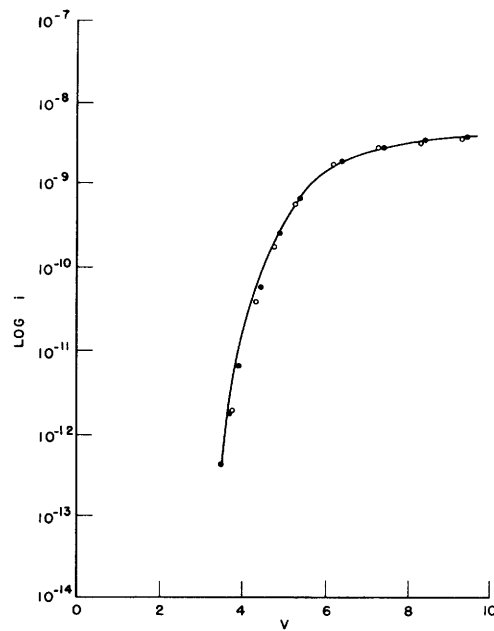


Fig. 12  
Superposition of direct current and simulated direct current.

order of 7 volts, which hardly seems credible (17).

7. Reflection effect at the anode. One must presume that a reflection effect may occur at the anode. If we assume that the reflection coefficient for tantalum is of the same general nature as that found by Nottingham (8) for tungsten and thoriated tungsten, then electrons approaching the anode at the top of its potential barrier will be completely reflected, and the reflection coefficient will fall away rapidly for increasing electron energy. If these reflected electrons return to the cathode, which is possible when the cathode and anode have comparable radii, then the retarding potential plot will be distorted. On the other hand, if a filamentary emitter is used, it will be likely that the reflected electrons may be able to make several excursions to the anode and finally be collected there. Therefore, the filamentary construction tends to eliminate anode reflection effects. For the same reasons, it is also true that the filamentary emitter will tend to make the anode appear to have a uniform work-function equal to its lowest value.

8. Patchy cathode. Patches could conceivably explain the shape of the experimental curve, but they could never explain the shift toward accelerating voltages. As we pointed out before, the shift could not be explained on a patch basis except by assuming that part of the cathode has a negative work-function. Furthermore, even the shape of the curve cannot be explained without unbelievable variations of patch size and patch potential.

The Schottky accelerating potential plots, which are presented later, could be approximated by Nottingham's (8) strip theory, using a patch size of  $2 \times 10^{-6}$  m and a work-function variation of 0.4 volt. Let us assume a model such that the cathode is divided into 9 parts whose work-functions run from  $\phi$  to  $\phi + 0.4$  in equal steps. Let us ignore the fields between patches and assume that the current reaching the collector is a summation of the currents from the individual patches. This is a crude model, for patch fields will decrease the collection current. However, if the strip theory were used, the difference in the strip-theory current from that of the Schottky theory would be no more than a factor of 2. This is because the transmission coefficient for the strip theory never falls below one-half, even for electrons whose kinetic energy is just equal to the mean-barrier height (17).

The results of the patch-theory calculation are presented in Fig. 13, together with the Schottky-theory curve. These results may be compared with Fig. 9, which presents the Schottky-theory curve and the curve using Nottingham's tungsten-reflection coefficient at 500°K. It is clear that the effect due to patches is almost negligible in comparison with the retarding potential curves of Figs. 5 through 8.

9. Reflection effect at the cathode. It has already been shown that Nottingham's reflection coefficient is unable to explain the experimental results found here. As in the case for patches, reflection effect could not explain the shift of the retarding potential curve to higher accelerating voltages, for such an explanation would require parts of the cathode to have a negative work-function. Although reflection effects may be

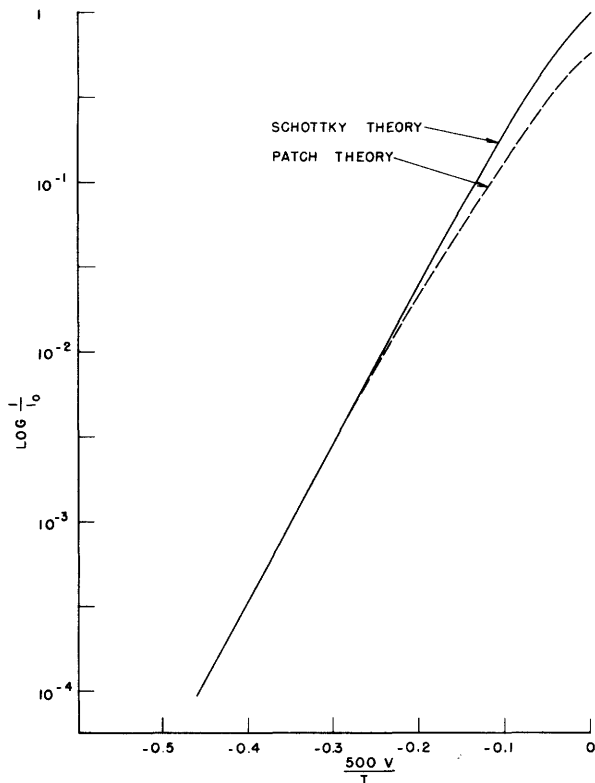


Fig. 13  
Comparison of Schottky theory  
and patch theory.

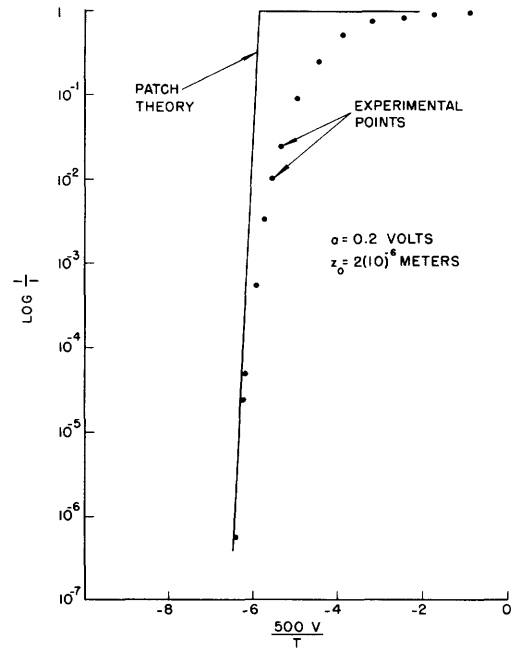


Fig. 14  
Retarding potential plot  
and patch theory.

present, they are undoubtedly small compared to the observed effects.

10. Crystallographic structure of the base metal. The work on projection tubes which was presented earlier indicates the absence of any effect on the emission from the crystallographic structure of the base metal. Even if such effects were present, they would only tend to make the cathode seem more patchy. As was shown above, the observed patch effects were negligible when compared with the experimental results.

11. Coating resistance. The remaining conceivable mechanism to explain the observed curves is that of a potential drop through a high resistance coating. The potential drop could cause both the broadening of the observed curves and a shift toward higher accelerating potentials, for such a drop would cause the actual potential difference between the oxide surface and the collector to be less than the applied voltage. Consequently, the applied voltage could be somewhat accelerating and there would still be a retarding voltage across the tube. The coating-resistance mechanism will be assumed in the analysis which follows. The results will be shown to be reasonable when compared with those of previous workers. Furthermore, this analysis leads to a useful method for studying coating resistance without the disadvantage of the disturbing influence of imbedded probes.

In Fig. 14 a typical retarding potential plot has been fitted with the patch-modified

Schottky theory. There is some doubt as to how the fit should be made. In the first place, the saturation current of the experimental points is slightly in doubt. Secondly, since the slope of the experimental curve is always less than that demanded by theory, the fit by horizontal translation could be in doubt by 0.3 volt. However, the best fit was made to the curves in turn, and the coating current was determined as a function of the coating voltage. For any current, the coating voltage will be given by the horizontal distance separating the two curves.

The resulting  $i$ - $V$  plots are presented in Fig. 15. These plots show nonlinearity in that  $di/dV$  increases for increasing emission current. Mutter (12) has observed such curves in a comparable temperature range, although the curvature was not nearly so marked. His curves were symmetrical about the origin, and at least part of the effect could be attributed to joule heating. It is difficult to see how the present results could be explained on this basis, since no time effects were observed and, at the highest current shown on Fig. 15, only  $1.7 \times 10^{-9}$  watt of power was being dissipated in the coating.

Although the nature of the experiment precludes taking data for the reverse direction of current, the curvature suggests rectification, and therefore the data were applied to Fan's rectification theory (18). According to this theory, the relation between  $i$  and  $V$  is given by

$$v = \frac{r^{1/2}}{3} \left[ \left( 2\ell + \frac{r}{p_o} \right)^{3/2} - \left( \frac{r}{p_o} \right)^{3/2} \right] \quad (4)$$

where

$$r = \frac{i}{2ebN^{3/2} (\pi kT/K)^{1/2}}$$

$$v = eV/kT$$

$$\ell = \frac{L}{(1/2e)N^{-1/2} (KkT/\pi)^{1/2}}$$

$$p_o = n_o/N$$

$i$  = current

$b$  = electron mobility

$K$  = dielectric constant of the insulating layer

$N$  = unit of density of electrons

$n_o$  = density of current carriers where the current enters the interface.

For the purposes of calculation it is easier to replace Eq. 4 by

$$V = Ai^{1/2} \left[ (B + i)^{3/2} - i^{3/2} \right] \quad (5)$$

where A and B depend on the quantities defined under Eq. 4. The points indicated on Fig. 15 have been computed, using Eq. 5. It was found that V was very insensitive to B, but depended heavily on A. It is seen that the i-V curve is well represented by theory at 536°K, not quite so well at 563°K, and only fairly well at 585°K. It is quite evident, however, that the i-V curves have the shape one would expect if an interface of high resistance were present. The presence of interface compounds is confirmed by the X-ray diffraction studies described later.

For small V, the conductivity will be proportional to  $\exp(-e\phi/kT)$  where  $\phi$  is the height of the interface barrier. The conductivity is computed from the slope of the i-V curves modified by a geometrical factor which depends on the radius of the base metal and the radius of the interface-oxide boundary. Since the thickness of the interface is unknown, it was assumed to be equal to the coating thickness for rough calculation. This will only multiply the conductivity by a constant factor and will not affect the determination of  $\phi$ .

In Fig. 16,  $\log \sigma$  vs  $1000/T$  is plotted for V near zero. The line is straight within the accuracy of the experiment, and the slope indicates a barrier height of 1.3 volts.

One must also ask if the conductivities found are of a reasonable order of magnitude. Although no data are available, we may compare the results of Fig. 16 with Eisenstein's (5) data for a  $Ba_2SiO_4$  interface. Extending his results to 600°K, the conductivities of the  $Ba_2SiO_4$  are found to run between  $10^{-11}$  mho/cm and  $10^{-14}$  mho/cm. Figure 16 shows that at 585°K the conductivity of the experimental coating is of the order of  $5 \times 10^{12}$  mho/cm.

Finally the results of Fan (14) and Hung (15) must be explained, for both of these workers presented retarding potential plots which approached closely to theory. Hung's base metal was grade-A nickel, which has been found to show very little rectifying action at the interface (19). Fan does not specify the grade of nickel used in his cathode, but his curves show he could have had no trouble with interface. Using again the data of Eisenstein (5), one finds that well-activated (BaSr)O has a much higher conductivity than the interface material  $Ba_2SiO_4$ , and a much lower conductivity activation energy. In fact, if Eisenstein's curves are extrapolated to 500°K, the conductivity is found to be approximately  $3 \times 10^{-4}$  mho/cm. This indicates that Fan and Hung, since they drew about the same currents as were drawn in the work reported here, would have coating voltage drops approximately  $10^{-8}$  as large. Their results would therefore not be expected to show interface difficulties.

#### E. Schottky Data

The accelerating field measurements were made with applied voltages running as high as 1200 volts. Because of the small filament radius this highest voltage represented a field, as determined by the microscopic geometry of the tube, of



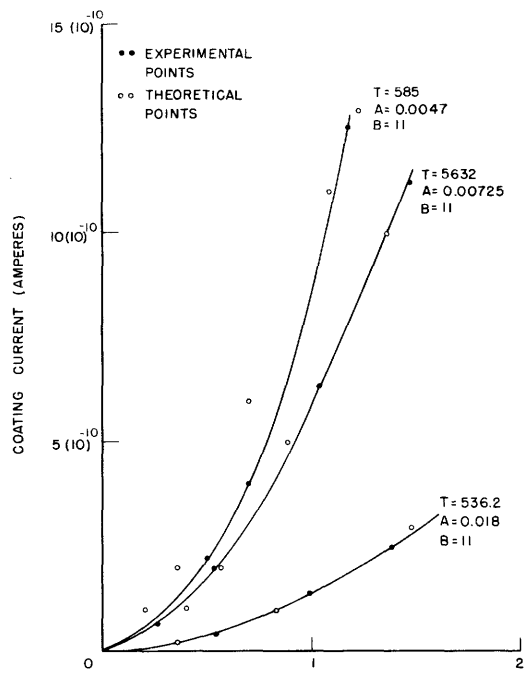


Fig. 15  
i-V curves.

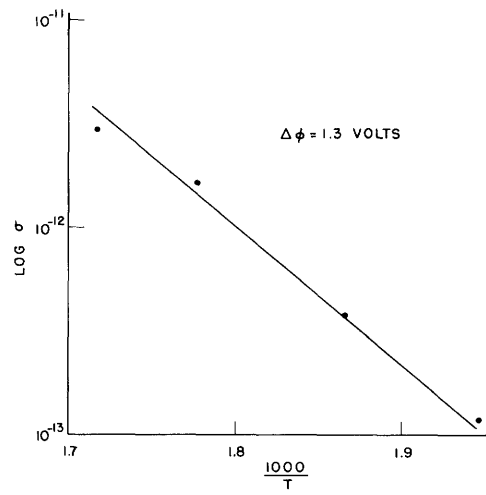


Fig. 16  
Conductivity plot.

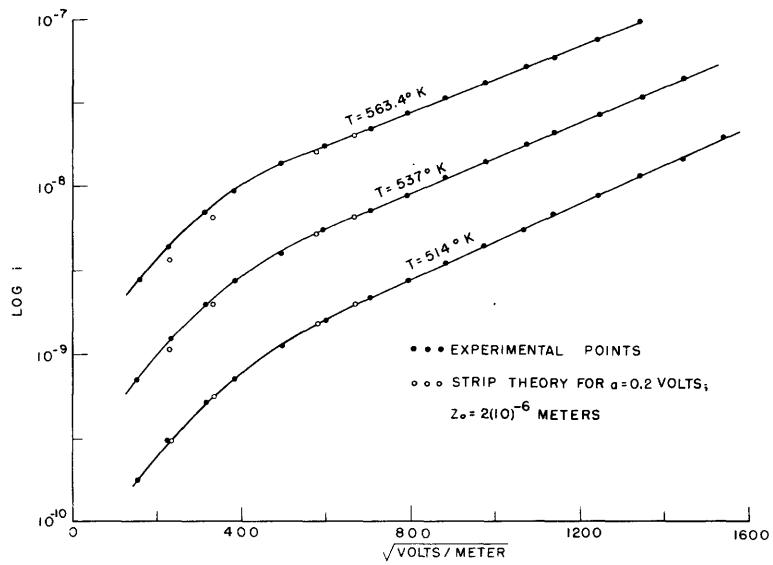


Fig. 17  
Schottky plot.

$2.6 \times 10^6$  volts/m. As will be shown later, the irregularities of the cathode surface caused an actual field of approximately  $1.9 \times 10^7$  volts/m.

Direct current was used to heat the filament and was supplied by well-insulated storage batteries. The filament current was measured by the type-K potentiometer (with the accelerating voltage removed). During any run, the constancy of the filament temperature could be observed with the photoelectric ammeter. If the circuit was well warmed up, the heating current did not vary during a run by more than 0.1 percent. The accelerating potentials were supplied by batteries up to 180 volts, by a regulated power supply to 500 volts and by another regulated supply up to 1200 volts. Curves were run at temperatures running from  $514^\circ\text{K}$  to  $563.4^\circ\text{K}$ . The highest current drawn was approximately  $10^{-6}$  amp/cm<sup>2</sup>. It was felt inadvisable to go to higher currents, since this might have changed the state of activation of the cathode, and it was desired to have all measurements pertain to the same activation.

The experimental curves are presented in Fig. 17. It is found that the currents rise quite rapidly up to applied fields of approximately  $2.5 \times 10^5$  volts/m, then become linear within experimental error up to the highest fields used. The slopes of the straight-line portions of the curves are higher than predicted by Schottky mirror-image theory, in each case by a factor of very nearly 3. Both of these facts must be explained.

Although the filament was coated cataphoretically, and thus is much smoother than a sprayed cathode, it is not reasonable to suppose that the cathode is smooth microscopically. The particle size of the coating suspension was approximately  $2.5 \times 10^{-6}$  m, and edges could be expected with radii of curvature several times smaller than this.

Schottky (20) has estimated the effect of surface irregularities by using as a model a pile of infinitely long half-cylinders on a plane. Each half-cylinder is superimposed by another of half its radius. If we let  $E_a$  be the applied field and  $E_e$  the effective field, then Schottky's results may be tabulated:

No. of half-cylinders		$E_e/E_a$
1	greater than	2
2	greater than	$2^2$
3	greater than	$2^3$

If these results were applied to the present cathode, the radii of the first three cylinders could be  $1.3 \times 10^{-6}$  m,  $3.3 \times 10^{-7}$  m, and  $6.5 \times 10^{-7}$  m, respectively. The dimensions are quite reasonable and could account for a field ratio of more than 8. On the basis of this approach it is proper to suppose that a fraction of the surface is subjected to fields much larger than the macroscopic field. Although the fraction of the area so affected may be small, the current is sufficiently field-sensitive that the preponderance of the emission will come from the small areas. Since the slopes of the Schottky plots

are high by a factor of approximately 3, we may say that the actual field is higher than the applied field by a factor of 9.

Nottingham's (8) strip theory was used to show that the slow rise of current at low fields could be explained by patches of reasonable size and reasonable voltage variation. According to this theory the work-function varies sinusoidally along one direction of the cathode surface and is constant in the orthogonal direction. The amplitude of the voltage variation is  $a$  and the period is  $z_0$ . The motive of an electron at any point between the emitter and the collector depends on the patch field, the image field, and the applied field. Those electrons escape whose motion is such that the energy associated with momentum away from the surface is at least as great as the maximum value of the motive for that direction.

By cut-and-try, the constants found to fit best the curve at  $T = 514^\circ\text{K}$  were  $a = 0.2$  volt and  $z_0 = 2 \times 10^{-6}$  m. The actual field was considered as 9 times the applied field for the reasons given above. The results of the calculation are shown as the hollow points on Fig. 17. By the nature of the theory, the computed points are obliged to fit in the straight-line section of the curve and so have not been put on the graph. It will be seen that the fit is excellent at the low temperature, and only slightly less satisfactory at  $T = 563^\circ\text{K}$ . Since the computed points are very sensitive to  $a$ , the value of 0.2 volt is probably very close to the correct one.

We must inquire why the Schottky plots of Fig. 17 show negligible effect of coating resistance. An examination of Fig. 15 shows that the conductivity of the curve for  $T = 563^\circ\text{K}$  changes from approximately  $2 \times 10^{-12}$  mho/cm to  $5 \times 10^{-11}$  mho/cm as the coating voltage runs from 0 volt to 1.5 volts and is still increasing. According to Fan (18), the effect of the blocking layer should disappear as the current increases, and the resistance of the layer should drop to that value which would occur if the interface were comparable to the oxide proper. Even if the conductivity increased only linearly with voltage, the coating drop at  $T = 563^\circ\text{K}$  and at the highest current drawn would be only 1.2 percent of the applied voltage. Actually, from Fan's discussion, the coating drop is probably small compared to the applied voltage.

The drop through the coating, if appreciable, should affect the Schottky plots by shifting them slightly to the right and broadening the low voltage section. This would mean that  $a/z_0$ , as computed above, would be slightly too large, but only slightly, because of the sensitivity of the fit on  $a$ .

Since  $a$  represents the amplitude of the sinusoidal variation of the work-function, the total variation would be twice the amplitude or 0.4 volt. It is on the basis of this analysis that the patch model for retarding fields was set up in which the work-function was assumed to vary in equal steps from  $\phi$  to  $\phi + 0.4$  volt.

#### F. X-ray Diffraction Study

Since all evidence so far accumulated points strongly to the presence of a high resistance interface, it was thought desirable to make an X-ray diffraction study of a

cathode of this type. This was done, using a filament prepared in a manner similar to that used on the one under discussion. Because of the small size of the filament, it proved impractical to separate the outer coating and the interface from the tungsten and make a powder pattern of the interface material. Instead, a small sample of the entire filament was mounted in a Debye camera. The sample was rocked back and forth, and exposed for 12 hours to copper-K $\alpha$  radiation. The result of the exposure was a series of lines representing the powder pattern of the coating superimposed on isolated spots from the single-crystal tungsten. The spots of the tungsten pattern were very sharp and symmetrical; this indicated the presence of a good single crystal, well-oriented with the axis of the wire.

The interface compounds of this study were originally reported (21) to be BaWO<sub>3</sub> and (BaSr)WO<sub>3</sub> with lattice parameters of 4.30 kX and 4.24 kX, respectively. These results were in agreement with those of Affleck and Hensley (22). However, Rooksby and Steward (23) have since reported the presence of Ba<sub>3</sub>WO<sub>6</sub> and Ba<sub>2</sub>SrWO<sub>6</sub> with lattice parameters of 8.6 kX and 8.5 kX, respectively. These last results have been confirmed by further work of Affleck and Hensley (24). On the basis of the above, the data were re-examined and the readily measurable lines were found consistent with either interpretation.

#### IV. Conclusion

Thermionic emission from oxide-coated tungsten filaments has been measured. It was found that the retarding potential data could best be interpreted as due to the presence of a high-resistance interface. Such an interpretation led to methods of analysis yielding the properties of this interface.

#### Acknowledgment

The author wishes to express his deep appreciation to Prof. Wayne B. Nottingham for suggesting this work and for his continual interest and help during its progress.

## References

1. A. Wehnelt: *Ann. Physik* 14, 425, 1904
2. K. B. Blodgett, I. Langmuir: *Rev. Sci. Instr.* 5, 321, 1934
3. R. P. Johnson, A. B. White, R. B. Nelson: *Rev. Sci. Instr.* 9, 253, 1938
4. M. H. Nichols: *Phys. Rev.* 57, 297, 1940
5. A. Eisenstein: *Advances in Electronics*, Academic Press, 1948
6. I. Langmuir, S. McLane, K. B. Blodgett: *Phys. Rev.* 35, 478, 1930
7. H. A. Jones, I. Langmuir: *Gen. Elec. Rev.* 310-319, 354-361, 408-412, 1927
8. W. B. Nottingham: *Phys. Rev.* 49, 78, 1936
9. W. B. Nottingham: *Phys. Rev.* 41, 793, 1932
10. J. P. Blewett: *J. Appl. Phys.* 10, 831, 1939
11. G. W. Mahlman: *J. Appl. Phys.* 20, 197, 1949
12. W. E. Mutter: *A Study of the Electronic Energy Level Structure of the Oxide-Coated Cathode*, Doctoral Thesis, Dept. of Physics, M.I.T. 1949
13. W. Schottky: *Ann. Physik* 44, 1011, 1914
14. H. Y. Fan: *J. Appl. Phys.* 14, 552, 1943
15. C. S. Hung: *J. Appl. Phys.* 21, 37, 1950
16. I. Langmuir: *Phys. Rev.* 2, 450, 1913
17. C. Herring, M. H. Nichols: *Revs. Modern Phys.* 21, 185, 1949
18. H. Y. Fan: *Phys. Rev.* 74, 1505, 1948
19. A. Fineman, A. Eisenstein: *J. Appl. Phys.* 17, 663, 1946
20. W. Schottky: *Z. Physik* 14, 63, 1928
21. C. P. Hadley: *A Study of Thermionic Emission from Fine Grain Oxide-Coated Emitters of Filamentary Dimensions*, Doctoral Thesis, Dept. of Physics, M.I.T. 1950
22. J. H. Affleck, E. B. Hensley: *J. Appl. Phys.* 21, 938L, 1950
23. H. P. Rooksby, E. G. Steward: *J. Appl. Phys.* 22, 358L, 1951
24. J. H. Affleck, E. B. Hensley: *J. Appl. Phys.* 22, 359L, 1951

